









RESEARCH PAPER

Natural variation in the adjustment of primary metabolism determines ammonium tolerance in the model grass *Brachypodium distachyon*

Marlon De la Peña^{1,†}, Théo Poucet^{1,2}, Francesc Montardit-Tarda³, Leyre Urmeneta¹, Jose Alberto Urbano-Gómez¹, Cédric Cassan², Izargi Vega-Mas¹, Pilar Catalán⁴, Ernesto Igartua³, Yves Gibon², M. Begoña Gonzalez-Moro¹, and Daniel Marino^{1,*}

¹ Department of Plant Biology and Ecology, University of the Basque Country (UPV/EHU), E-48940, Leioa, Spain

² Université de Bordeaux, INRAE, UMR Biologie du Fruit et Pathologie, Bordeaux Metabolome, F-33140 Villenave d'Ornon, France

³ Department of Genetics and Plant Breeding, Aula Dei Experimental Station, CSIC, Avda Montañana 1005, 50059 Zaragoza, Spain

⁴ Escuela Politécnica Superior de Huesca, Universidad de Zaragoza, Ctra. Cuarte km 1, 22071 Huesca, Spain

[†] Present address: School of Plant Sciences, University of Arizona, Tucson, AZ, USA

* Correspondence: daniel.marino@ehu.eus

Received 30 April 2024; Editorial decision 4 September 2024; Accepted 17 September 2024

Editor: Stanislav Kopriva, University of Cologne, Germany

Abstract

Nitrogen (N) fertilization is essential to maximize crop production. However, around half of the applied N is lost to the environment, causing water and air pollution and contributing to climate change. Understanding the natural genetic and metabolic basis underlying plants N use efficiency is of great interest to attain an agriculture with less N demand and thus more sustainable. The study of ammonium (NH₄⁺) nutrition is of particular interest, because it mitigates N losses due to nitrate (NO₃⁻) leaching or denitrification. In this work, we studied *Brachypodium distachyon*, the model plant for C₃ grasses, grown with NH₄⁺ or NO₃⁻ supply. We performed gene expression analysis in the root of the *B. distachyon* reference accession Bd21 and examined the phenotypic variation across 52 natural accessions through analyzing plant growth and a panel of 22 metabolic traits in leaf and root. We found that the adjustment of primary metabolism to NH₄⁺ nutrition is essential for the natural variation of NH₄⁺ tolerance, notably involving NH₄⁺ assimilation and phosphoenolpyruvate carboxylase (PEPC) activity. Additionally, genome-wide association studies (GWAS) indicated several loci associated with *B. distachyon* growth and metabolic adaptation to NH₄⁺ nutrition. We found that the *GDH2* gene was associated with the induction of root glutamate dehydrogenase activity under NH₄⁺ nutrition and that two genes encoding malic enzyme were associated with leaf PEPC activity. Altogether, our work underlines the value of natural variation and the key role of primary metabolism to improve NH₄⁺ tolerance.

Abbreviations: CS, citrate synthase; FK, fructokinase; GDH, glutamate dehydrogenase; GK, glukokinase; GOGAT, glutamate synthase; GS, glutamine synthetase; GWAS, genome-wide association study; ICDH, NADP-dependent isocitrate dehydrogenase; MDH, malate dehydrogenase; ME, malic enzyme; NUE, nitrogen use efficiency; OPLS-DA, orthogonal projection to latent structures-discriminant analysis; PCA, principal component analysis; PEPC, phosphoenolpyruvate carboxylase; PK, pyruvate kinase; TCA, tricarboxylic acid.

© The Author(s) 2024. Published by Oxford University Press on behalf of the Society for Experimental Biology.

This is an Open Access article distributed under the terms of the Creative Commons Attribution-NonCommercial-NoDerivs licence (<https://creativecommons.org/licenses/by-nc-nd/4.0/>), which permits non-commercial reproduction and distribution of the work, in any medium, provided the original work is not altered or transformed in any way, and that the work is properly cited. For commercial re-use, please contact reprints@oup.com for reprints and translation rights for reprints. All other permissions can be obtained through our RightsLink service via the Permissions link on the article page on our site—for further information please contact journals.permissions@oup.com.

Keywords: Ammonium, *Brachypodium*, glutamate dehydrogenase, GWAS, metabolism, natural variation, nitrate, nitrogen, nutritional stress, phosphoenolpyruvate carboxylase.

Introduction

Crop grasses, including cereals, play a critical role in human nutrition, while also serving as a crucial component of animal feed and biofuel production. The optimization of crop yield relies heavily on nitrogen (N), resulting in the annual usage of >100 Mt of N fertilizers (Swarbreck *et al.*, 2019). However, N use efficiency (NUE), which measures the proportion of applied fertilizer that is recovered in grain, is estimated to be between 30% and 50%. A low NUE means a significant amount of N is lost to the environment, with an estimation of 50 kg N ha⁻¹ year⁻¹ lost through leaching and greenhouse gas emissions that negatively affect water and air quality and contribute to climate change (Lassaletta *et al.*, 2016; Coskun *et al.*, 2017; Swarbreck *et al.*, 2019).

Non-leguminous vascular plants mainly obtain N from the absorption of ammonium (NH₄⁺) or nitrate (NO₃⁻), primary N sources present in fertilizers. NH₄⁺ is directly assimilated into organic compounds while NO₃⁻ has to be first reduced to NH₄⁺ to be used. In this sense, a higher content of assimilated N is a general feature of plants grown under NH₄⁺ nutrition (Esteban *et al.*, 2016; González-Moro *et al.*, 2021). The negative charge of NO₃⁻ prevents its adhesion to soil particles and thus is prone to leaching, which makes it unavailable for plant use and decreases the NUE of the agrosystem. In this regard, NH₄⁺-based fertilization in combination with a nitrification inhibition strategy, which blocks its oxidation by soil microbial nitrifiers, appears as a promising alternative to improve NUE since it maintains N in the soil for longer periods, and thus can reduce the amount of N fertilizer needed. Adopting this approach leads to reduced NO₃⁻ leaching and N₂O emissions when compared with a more nitric fertilization (Subbarao and Searchinger, 2021; Xiao *et al.*, 2023). However, an excessive concentration of NH₄⁺ in the soil can lead to plants suffering stress. The most common symptoms of NH₄⁺ stress are reduced plant growth and altered root architecture compared with plants grown with NO₃⁻ supply. When NH₄⁺ stress increases because of the high NH₄⁺ concentration and/or the length of exposure, symptoms become more severe and include leaf chlorosis and even plant death. The causes of this symptomatology are diverse and comprise oxidative stress, intracellular pH alterations, and unbalanced mineral nutrition (Britto and Kronzucker, 2002; Coletto *et al.*, 2023; Xiao *et al.*, 2023). These adverse effects are commonly attributed to the excessive NH₄⁺ uptake, accumulation, or even assimilation (Britto and Kronzucker, 2002; Sarasketa *et al.*, 2014; Hachiya *et al.*, 2021).

Although NH₄⁺ stress is considered universal, the threshold concentration of NH₄⁺ to trigger stress varies between plant

species. Some species, such as *Spinacia oleracea* (Lasa *et al.*, 2002), display very high sensitivity to NH₄⁺, whereas species such as oil palm are highly tolerant (De la Peña *et al.*, 2023). In addition, important variability has been reported within the same species such as *Arabidopsis thaliana* (Sarasketa *et al.*, 2014; Chen *et al.*, 2021; Katz *et al.*, 2022), pea (Cruz *et al.*, 2011), or rice (Di *et al.*, 2018). In general, plants adapted to low nitrification environments show the highest tolerance to NH₄⁺ stress, such as late-successional conifers adapted to acidic soils (Britto and Kronzucker, 2013), rice to paddy fields with limited oxygen availability (Xiao *et al.*, 2023), and species such as the C₄ grass *Spartina alterniflora* adapted to saline soils (Hessini *et al.*, 2013). In agricultural soils, nitrification is very active, and thus crops have been bred for their ability to grow using NO₃⁻ as primary N source regardless of the fertilizer used. Thus, many crops could have lost their ability to efficiently handle NH₄⁺ nutrition. In this sense, exploiting natural variability in order to identify traits to enhance NH₄⁺ tolerance is of great interest, notably in wild species that have not been subjected to a nitrifying environment.

Brachypodium distachyon is a wild C₃ grass that belongs to the *Pooideae* subfamily and is closely related to important cereal crops such as barley and wheat (Kellogg, 2015; Catalan *et al.*, 2016; Scholthof *et al.*, 2018). Its reduced diploid genome, small size, and short generation time make it an attractive and powerful model for research. Importantly, many common features with cereals have been revealed, such as biotic stress responses and cell wall composition, and even its root microbiome and root exudate profile closely resemble those of wheat (Hasterok *et al.*, 2022). Importantly, several works validated *B. distachyon* as a model to study N nutrition in cereals, for instance studying the dynamics of NO₃⁻ uptake (David *et al.*, 2019). Regarding NH₄⁺ nutrition, we reported that the reference accession *B. distachyon* Bd21 displayed a similar metabolic behavior upon NH₄⁺ stress compared with wheat, for example accumulating NH₄⁺ and asparagine in roots and diverting carbon (C) metabolism to facilitate NH₄⁺ assimilation (De la Peña *et al.*, 2019). Overall, the study of N nutrition in *B. distachyon* fills a gap with cereals compared with the use of *Arabidopsis thaliana* with dicot crops, all while keeping the advantages of working with a model plant. For instance, differences have been observed between these two models regarding NRT2 NO₃⁻ transporters (Wang *et al.*, 2018) or plant metabolic performance upon NH₄⁺ nutrition (De la Peña *et al.*, 2019). Advancing towards the identification of the genetic and metabolic basis of the adaptation to ammonium nutrition in monocots is of great interest to improve the ammonium use efficiency of cereals that

will help make agricultural systems more sustainable, notably regarding N losses.

In this context, we studied the non-domesticated grass model *B. distachyon*, performing a transcriptomic analysis in the reference accession Bd21 and surveying the responses towards NH_4^+ stress in 52 natural accessions collected throughout its native growth range in the Mediterranean and the Middle East that were previously used to build the *B. distachyon* pan-genome (Gordon *et al.*, 2017). All accessions were grown in hydroponic conditions with NO_3^- or NH_4^+ as N source. Plant growth and 22 metabolic markers (13 metabolites and nine enzyme activities) were determined in both roots and leaves. We examined the obtained phenotypic data with multivariate analyses to elucidate the involvement of metabolic adaptation in NH_4^+ tolerance in grasses. Furthermore, combining the acquired data with genomic information, we conducted a genome-wide association study (GWAS), a genetic approach tailored to investigate complex and polygenic traits. This method facilitated the identification of potential regulatory genetic loci associated with NH_4^+ nutrition, helpful for the development of cereal cultivars with a more efficient use of NH_4^+ as the source of N.

Materials and methods

Plant growth and experimental design

Seeds were washed in a solution containing 15% bleach and 0.1% Triton X-100 for 4 min, followed by thorough rinsing with sterile deionized water. To synchronize germination, seeds were placed on damp sterile filter paper in Petri dishes and stratified in darkness at 4 °C for 7 d. After stratification, plates were transferred to a growth chamber and kept in the dark for an additional 3 d. Germinated seeds were sown on trays filled with perlite:vermiculite (1:1, v:v) soaked with deionized water. After 7 d, homogeneous seedlings were selected and transferred to hydroponic tanks.

For transcriptomic analysis, 12 seedlings of the *B. distachyon* Bd21 reference accession were placed in tanks of 4.5 liters growing under ammonium or nitrate conditions (three tanks per condition). Plants were grown during 19 d with 2.5 mM N, a N-sufficient condition as established in De la Peña *et al.* (2019) supplied as 1.25 mM $(\text{NH}_4)_2\text{SO}_4$ or 1.25 mM $\text{Ca}(\text{NO}_3)_2$. In addition, the nutrient solution contained 1.15 mM K_2HPO_4 , 0.85 mM MgSO_4 , 0.7 mM CaSO_4 , 2.68 mM KCl, 0.5 mM CaCO_3 , 0.07 mM NaFeEDTA, 16.5 μM Na_2MoO_4 , 3.7 μM FeCl_3 , 3.5 μM ZnSO_4 , 16.2 μM H_3BO_3 , 0.47 μM MnSO_4 , 0.12 μM CuSO_4 , 0.21 μM AlCl_3 , 0.126 μM NiCl_2 , and 0.06 μM KI. To properly compare both N sources, NO_3^- -fed plants were supplied with 1.25 mM CaSO_4 to match the SO_4^{2-} supplied with the NH_4^+ . The pH was 6.8 and its stability was checked every 2 d with a pHmeter and maintained in ± 0.2 units during the whole experiment. The nutrient solution was replaced every 4 d. The individuals grown in the same tank were pooled and considered as a biological replicate, immediately frozen in liquid nitrogen, ground to powder using a Tissue Lyser (Retsch MM 400) at cryogenic temperature, and stored at -80 °C until RNA extraction.

To characterize the intraspecific variability in the metabolic adaptation of *B. distachyon* to nitrate or ammonium nutrition, we analyzed 52 accessions that were *de novo* assembled and annotated by Gordon *et al.* (2017) (<https://brachypan.jgi.doe.gov/>). To do so, we employed 1.2 liter tanks, each accommodating three seedlings of a single accession (three tanks per accession). The growth conditions and medium composition were the same as for the transcriptomic analysis. Harvesting of the plants took

place between 10.00 h and 12.00 h, 2 h after the onset of the light period. Shoots and roots were separated and weighed individually. The three individuals grown in the same tank were pooled together and considered as a biological replicate, immediately frozen in liquid nitrogen, ground to powder using a Tissue Lyser (Retsch MM 400) at cryogenic temperature, and stored at -80 °C until further use.

Metabolite determination

Ethanol extraction was carried out with 20 mg of frozen root or leaf powder in three phases. Samples were homogenized with 250 μl of 80% ethanol in 10 mM HEPES (pH 6), incubated for 20 min at 80 °C, centrifuged at 16 000 g for 5 min at 4 °C, and the supernatant was recovered. The process was repeated with 150 μl of 80% ethanol in 10 mM HEPES (pH 6), and with 250 μl of 50% ethanol in 10 mM HEPES (pH 6). The three supernatants were pooled together and the resulting pellet resuspended in 400 μl of 0.1 M NaOH to measure proteins and starch. Total chlorophyll, soluble sugars, citrate, malate, protein, and starch were determined as described in Poucet *et al.* (2021). The NH_4^+ and NO_3^- content was quantified as described in Sarasketa *et al.* (2014) and Tschoep *et al.* (2009), respectively. Total free amino acids were quantified as described by Bantan-Polak *et al.* (2001). Glutamate quantification was determined following Zhang *et al.* (2015), and total glutathione as described by Griffith (1980).

Enzyme activities

A 20 mg aliquot of frozen leaf and root powder was extracted by vigorous shaking with 500 μl of extraction buffer [20% (v/v) glycerol, 1% Triton X-100 (v/v), 50 mM HEPES-KOH (pH 7.5), 10 mM MgCl_2 , 1 mM EDTA, 1 mM EGTA, 1 mM aminocaproic acid, 1 mM benzamide, 20 μM leupeptin, 0.5 mM DTT, 1 mM phenylmethylsulfonyl fluoride, 10% polyvinylpyrrolidone (w/v)]. Glucokinase (GK), fructokinase (FK), glutamate dehydrogenase (GDH), phosphoenolpyruvate carboxylase (PEPC), malate dehydrogenase (MDH), pyruvate kinase (PK), total citrate synthase (CS), mitochondrial citrate synthase (CSm), and NADP-dependent isocitrate dehydrogenase (ICDH) enzyme activities were assayed by spectrophotometry with robotized microplate assays (Gibon *et al.*, 2004). The evolution of NAD(P)H was monitored at 340 nm after incubation at 25 °C. The activity of GDH was measured at 570 nm via a cycling reaction involving the reduction of 3-(4,5-dimethylthiazol-2-yl)-2,5-diphenyl tetrazolium bromide in the presence of alcohol dehydrogenase and phenazine ethosulfate. CS activity was measured at 412 nm following the reduction of 2 mM DTNB [5,5'-dithiobis(2-nitrobenzoic acid)] as described in Anoop *et al.* (2003). All assays have been validated by checking the recovery of a biological standard (tomato leaf extract) and by ensuring that the dilution of the extracts had no effect on the estimation of activities, as described in Bénard and Gibon (2016).

Transcriptomic analysis

Total RNA was isolated from 25 mg of Bd21 frozen root powder grown under NH_4^+ or NO_3^- nutrition using the Nucleospin RNA plant kit (Macherey-Nagel), which included DNase treatment. RNA quality was analyzed on Agilent RNA 6000 Nano chips in an Agilent 2100 Bioanalyzer (Agilent, Santa Clara, CA, USA). Three independent biological replicates were analyzed; each replicate corresponded to a pool of 12 plants. mRNA was purified using poly(T)oligo-attached magnetic beads. Libraries were generated with the NEBNext® Ultra™ RNA Library Prep Kit for Illumina® (NEB, USA) and sequenced, generating paired-end reads on an Illumina platform. Library preparation and sequencing were outsourced to Novogene (UK).

The sequencing reads were aligned to *B. distachyon* reference genome version 3.1, using the software HISAT2 (Kim *et al.*, 2019). Transcripts were quantified as fragments per kilobase of transcript per million mapped reads (FPKM) with HTseq (Anders *et al.*, 2015). Differential expression was assessed using the DESeq2 package (Love *et al.*, 2014). DESeq2 provides statistical routines for determining differential expression in digital gene expression data using a model based on the negative binomial distribution. *P*-values were adjusted using the Benjamini and Hochberg's approach for controlling the false discovery rate (FDR). Genes with an adjusted *P*-value <0.05 found by DESeq2 were assigned as differentially expressed. Gene ontology (GO) enrichment analysis was performed using g:Profiler (Kolberg *et al.*, 2023).

For quantitative PCR (qPCR) 1 µg of total RNA was retrotranscribed into cDNA (PrimeScript™ RT; Takara Bio) and gene expression was determined from 2 µl of a 1:10 cDNA dilution in a 15 µl reaction volume using TB Green® Premix Ex Taq™ II (Takara Bio) in a Step One Plus Real Time PCR System (Applied Biosystems). The PCR program was 5 min at 95 °C and 40 cycles of 94 °C for 15 s and 60 °C for 30 s. The relative expression levels of target genes were calculated by the $2^{-\Delta\Delta Ct}$ method where ΔCt is the difference in threshold cycle number (Ct) for the target gene and the mean of the reference genes *BdUBI10* and *BdEF11a*. Primers used are available in De la Peña *et al.* (2019) and in Supplementary Table S1.

Genome-wide association study

We performed GWAS on a dataset of 51 accessions using the Genome Association and Prediction Integrated Tool-R package (GAPIT version 3) (Wang and Zhang, 2021). The genetic diversity file (*Bdistachyon_314.vcf*) was obtained from Phytozome (Goodstein *et al.*, 2012). Biallelic single nucleotide polymorphisms (SNPs), mapped on reference assembly v3.0, were subsequently filtered to remove loci with missing calls in more than two accessions. This analysis was conducted for all measured phenotypes under NH_4^+ or NO_3^- nutritional conditions. GWAS analysis was performed with a multilocus mixed model (MLMM). Population structure was controlled with a kinship matrix (Supplementary Fig. S1A) and a principal component (PC) matrix of two dimensions (Supplementary Fig. S1B). The principal component analysis (PCA) and the kinship matrix were calculated from an SNP fraction of 0.05 (5% randomly selected markers). The first two dimensions of the PCA explained nearly 50% of marker variance, and indicated the presence of three populations. A threshold probability of 1×10^{-5} for individual tests was considered as significant. To ensure reliable associations, we removed SNPs with a low minor allelic frequency (MAF) <10% across the panel, as these SNPs can often lead to false-positive associations. In total, our analysis included 1 845 901 SNPs distributed across the five chromosomes of *B. distachyon*. Many marker–trait associations found were close in the physical map, indicating a common underlying gene. These close associations were grouped in single quantitative trait loci (QTLs) following a linkage disequilibrium (LD)-based method. First, LD, adjusted by kinship and PCs, was calculated with the LDcorSV package (Mangin *et al.*, 2012). Background LD was computed as the LD corresponding to the 95th percentile of a normal distribution fitted to the pairwise interchromosomal LD values computed for a random set of 200 markers per chromosome (1000 in total), after square root transformation as in Bresghele and Sorrells (2006). LD decay per chromosome was computed as the distance at which a Loess curve fitted to the set of pairwise LD values between 1000 random SNPs crossed the background LD. Marker–trait associations were identified as belonging to the same QTL if the associated SNPs were closer than the corresponding chromosomal LD distance. To search for candidate genes at each of the identified QTLs, we defined the confidence region for each QTL. To this end, LD decay of each QTL from the top associated SNP was calculated fitting a Loess curve to the pairwise LD values calculated with 1000 thinned SNPs, extracted from

the flanking region of ± 1 Mb. The confidence region was defined as the distance from the top SNP to the point where the Loess curve decreased to half of its maximum value, as in Vos *et al.* (2017).

Statistical analysis

All statistical analyses were performed using R (R version 4.2.2). PCA scores were generated with the FactoMineR package (Lê *et al.*, 2008), along with hierarchical clustering analysis (HCA) using the 'heatmap.2' function from the gplots package. To identify significant metabolic variables contributing to the separation of the top sensitive and tolerant accessions, PCA and orthogonal projection to latent structures-discriminant analysis (OPLS-DA) were carried out using the 'ropls' package (Thevenot *et al.*, 2015). For this purpose, the data were scaled using the Pareto method. To analyze variable individually, ANOVA was performed on the linear regression model, utilizing type III sums of squares. Additionally, for the total plant biomass, we calculated the estimated marginal means and compared the effects of NH_4^+ and NO_3^- nutrition in each genotype by performing post-hoc Tukey multiple comparisons using the 'emmeans' package (Lenth *et al.*, 2018). For each case, we ensured the validity of the assumptions by evaluating the normality and homogeneity of variance through the Kolmogorov–Smirnov and Levene's tests, respectively.

Results and discussion

The N source had extensive influence on root gene expression in *B. distachyon*

Brachypodium distachyon was previously described as a good model to study NH_4^+ nutrition, showing a similar behavior compared with other grasses and cereals (De la Peña *et al.*, 2019). In the present study, to further understand *B. distachyon* response to the N source provided, we performed a transcriptomic analysis in the root of the reference accession Bd21 grown with 2.5 mM NH_4^+ or NO_3^- supply. This N concentration represents an N-sufficient condition that, when supplied in the form of NH_4^+ , entails a stress situation that provokes growth impairment with respect to NO_3^- nutrition (De la Peña *et al.*, 2019, 2022). In the present work, a similar growth reduction phenotype was observed, as shown in Supplementary Fig. S2. Transcriptomic analysis revealed that long-term growing with exclusive NH_4^+ or NO_3^- as N source had a great impact at the root transcriptional level, with 2974 differentially expressed genes. Out of them, 1467 showed higher expression under ammonium nutrition while 1507 showed higher expression under nitrate nutrition (Supplementary Table S2). GO enrichment analysis revealed categories associated with oxidative stress such as 'response to oxidative stress', 'glutathione metabolic process', or 'hydrogen peroxide metabolic process', with iron homeostasis such as 'L-methionine biosynthetic process' and 'transition metal ion transport', and with C and N metabolism such as 'nitrate import', 'carboxylic acid metabolic process', and 'amino acid transmembrane transport' (Fig. 1; Supplementary Table S3). This general response is in agreement with previous reports that showed Fe homeostasis alteration under NH_4^+ nutrition

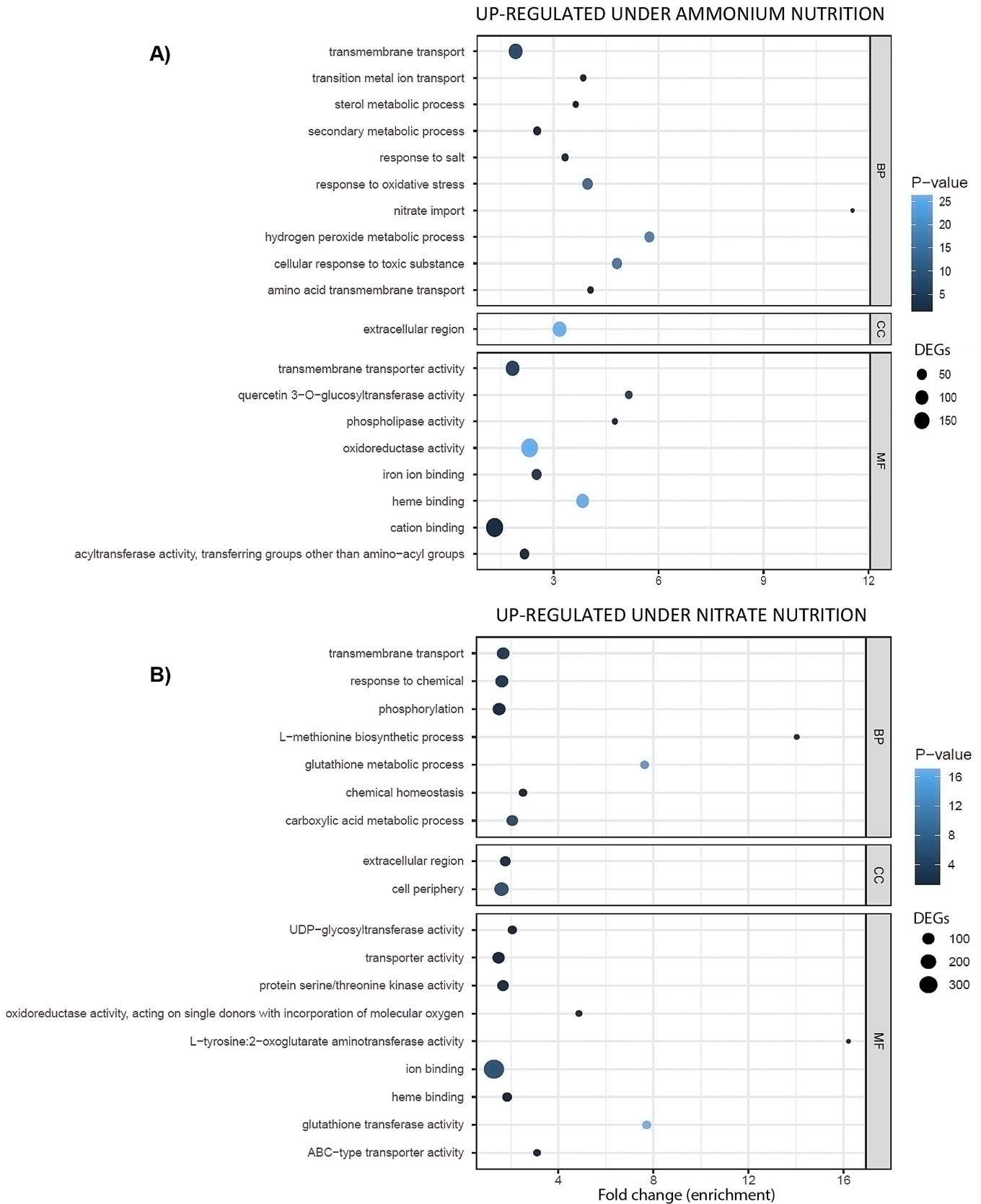


Fig. 1. Gene ontology (GO) enrichment analysis of differentially expressed genes (DEGs) [$P < 0.05$, fold change (FC) > 2] with higher expression in the root of ammonium-fed (A) or nitrate-fed (B) *Brachypodium distachyon* Bd21 plants. Only driver terms identified with g:Profiler are shown. BP, CC, and MF mean biological process, cellular component, and molecular function, respectively. The color scale represents the P -value given as $-\log_{10}$ and the dot size the number of DEGs within each category. All DEGs are shown in [Supplementary Table S2](#) and the whole GO analysis in [Supplementary Table S3](#).

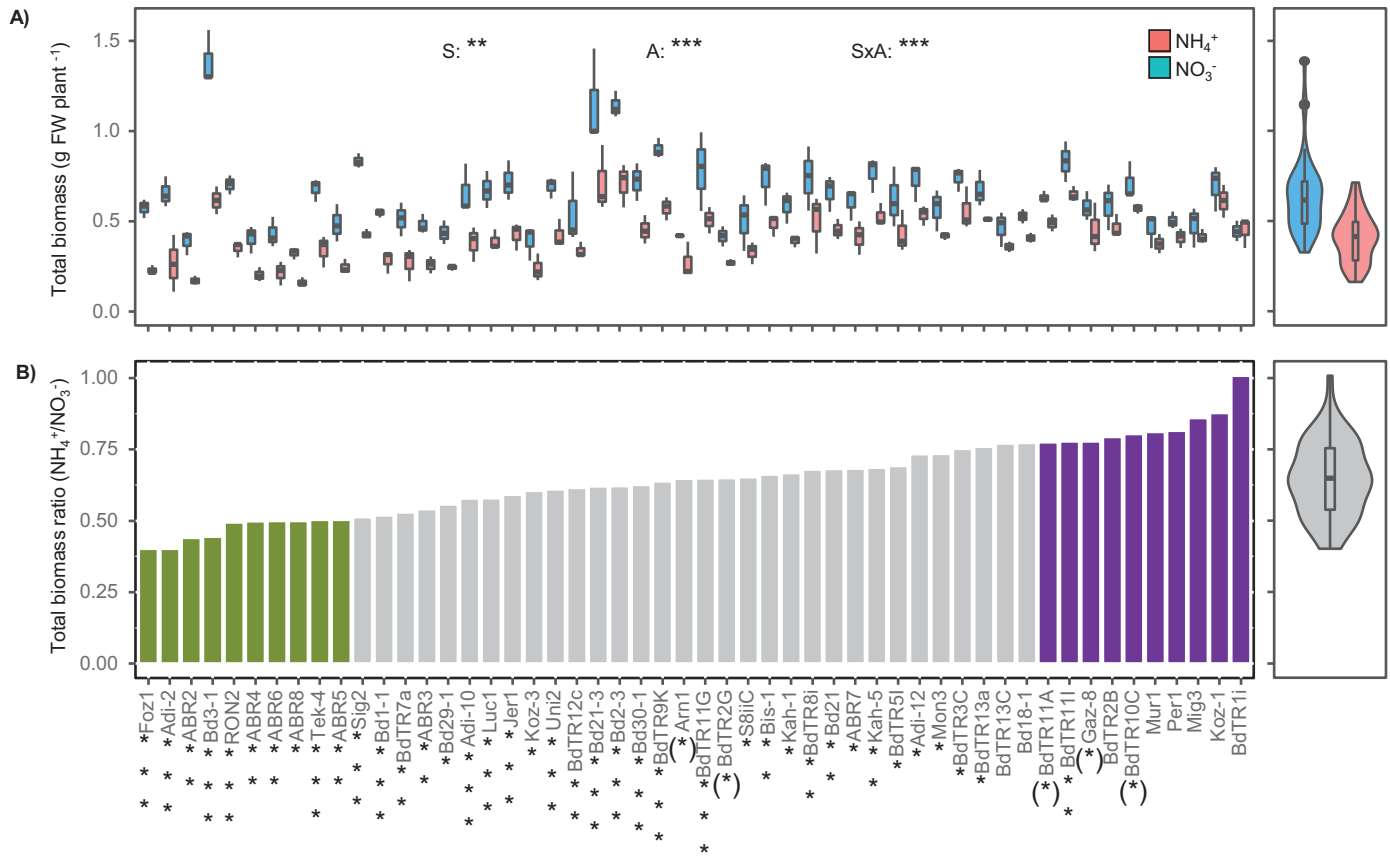


Fig. 2. Natural variation of 52 accessions of *B. distachyon* grown under nitrate or ammonium as N source. (A) Total plant biomass. (B) Ratio between total plant biomass mean under ammonium versus nitrate nutrition. For (A), values represent the mean \pm SE ($n=3$). Each biological replicate corresponds to three plants grown in the same tank. Violin plots on the right side show the overall distribution of the traits. Significant effects of N source (S), accession (A), and their interaction (SxA) from two-way ANOVA, as well as the significance of N source effect within each accession, are indicated ($*$) $P<0.1$, $*$ $P<0.05$, $**P<0.01$, $***P<0.001$). Red and blue color refer to ammonium and nitrate nutrition, respectively. The top 10 accessions displaying the highest tolerance and the highest sensitivity to ammonium nutrition are shown in purple and yellow, respectively.

in *B. distachyon* (De la Peña et al., 2022) and *Arabidopsis* (X.X. Liu et al., 2022; Y. Liu et al., 2022). Moreover, redox alterations are also common under NH_4^+ nutrition (Podgórska et al., 2013), among others in relation to Fe homeostasis (X.X. Liu et al., 2022). We looked in detail into the expression of genes coding for N transporters (Supplementary Table S4). Seven *NRT2* genes, four *NRT1;1* homologs, and two *AMT1* genes have been identified in the *B. distachyon* genome (Plett et al., 2010; Girin et al., 2014; von Wittgenstein et al., 2014). In our work, an N source effect was evident in the expression of N transporters, notably observing a great induction of *NRT2* members in nitrate-grown plants. Similarly, the gene expression of *AMT1* ammonium transporters was significantly higher under ammonium nutrition (Supplementary Table S4). Regarding C and N, it has been widely reported that NH_4^+ nutrition entails an important adaptation of primary metabolism that has an impact on plant tolerance. Among others, the induction of NH_4^+ assimilation is considered as an NH_4^+ tolerance-promoting mechanism (Kusano et al., 2011;

Guan et al., 2016). However, excessive NH_4^+ assimilation also demands an intense C supply derived from the tricarboxylic acid (TCA) cycle that leads to C–N imbalance and is considered as a trade-off for growth (Poucet et al., 2021; Kong et al., 2022). In fact, glutamine (Gln) synthesis and/or accumulation in plastids is associated with enhanced sensitivity to NH_4^+ stress in *Arabidopsis* (Hachiya et al., 2021) and rice (Xie et al., 2023).

Brachypodium distachyon displays extensive growth variation as a function of the available N source

To further study the response of *B. distachyon* to NH_4^+ nutrition, we performed a natural variation study comparing the performance of 52 natural accessions grown under exclusive NH_4^+ or NO_3^- supply. As markers of plant physiology, we determined shoot and root biomass and leaf chlorophyll content. Taking into consideration the available literature and the transcriptomic results, we focused on primary metabolism to

study the differential adaptation of the studied accessions to the N source provided and analyzed nine enzyme activities and 13 metabolites. The whole dataset generated for this work is available in [Supplementary Table S5](#).

Given that NH_4^+ nutrition represents a stress condition, the N source had a significant impact on plant biomass, with a general decrease in biomass accumulation for NH_4^+ -fed with respect to NO_3^- -fed plants ([Fig. 2A](#)). To allow comparison among genotypes, the total plant biomass ratio of the NH_4^+ versus the NO_3^- condition was employed, a parameter previously used as an NH_4^+ toxicity/tolerance indicator ([Ariz et al., 2011](#); [Sarasketa et al., 2014](#)). This ratio revealed extensive natural variation upon NH_4^+ tolerance in *B. distachyon*. The most sensitive accessions showed ratios below 0.5 and the most tolerant accessions close to 1 ([Fig. 2B](#)). The reference accession Bd21 showed an intermediate phenotype with a ratio of 0.68, in line with previous works ([De la Peña et al., 2019, 2022](#); [Glazowska et al., 2019](#)). The pattern for shoot and root biomass for these accessions was consistent with that of their respective total biomass ([Supplementary Fig. S3](#)).

Root metabolic adaptation determines *B. distachyon* intraspecific variability towards ammonium tolerance

In order to explore the distribution of the accessions with respect to the metabolic variables determined, a PCA was conducted considering all enzymes and metabolites with the exception of chlorophyll and starch, as they were not measured in roots. PC1 and PC2 explained 76% of the total variation. As expected, the PCA clearly differentiated root and leaf data ([Fig. 3](#)). Regarding the N source effect, the analysis also

discriminated NH_4^+ - and NO_3^- -grown plants. Notably, the impact of the N source on root metabolism was greater compared with leaf metabolism, as all the accessions were clearly separated into two non-overlapping clusters based on root data, while the two groups partially overlapped when considering the leaf data ([Fig. 3](#)), thus supporting a higher variation in root versus leaf metabolic response to NH_4^+ nutrition than to NO_3^- nutrition. The variables with a higher contribution to group separation along PC1 were nitrate, MDH, and CSm. Notably, nitrate had a great influence on the separation of root groups. The enzyme activities GK, FK, PK PEPC, ICDH, GDH, and CS were the variables with the highest contribution to the separation along PC2 ([Supplementary Fig. S4](#)). Looking at the general behavior of the metabolic variables individually across the studied accessions ([Supplementary Figs S5, S6](#)), the NO_3^- condition exhibited, as expected, significantly higher levels of tissue NO_3^- ([Supplementary Figs S5C, S6B](#)), while the NH_4^+ condition exhibited higher levels of tissue NH_4^+ , notably in the root ([Supplementary Fig. S6A](#)). A high NH_4^+ concentration stimulates its assimilation and, in agreement with this, the amino acid content was also higher in the leaves and root of NH_4^+ -fed *B. distachyon* accessions ([Supplementary Figs S5E, 6D](#)). In addition, protein content was also higher in the root ([Supplementary Fig. S6C](#)). C metabolism adaptation, among others to sustain the supply of C skeletons for amino acid synthesis, is also common under NH_4^+ nutrition. This C metabolic adaptation involves a redistribution of soluble sugars and the adjustment of the TCA cycle functioning to work in an open-flux mode, diverting C skeletons, mainly 2-oxoglutarate, for N assimilation. Under this circumstance, the action of the anaplerotic enzymes is of great importance to replenish the intermediates of the cycle.

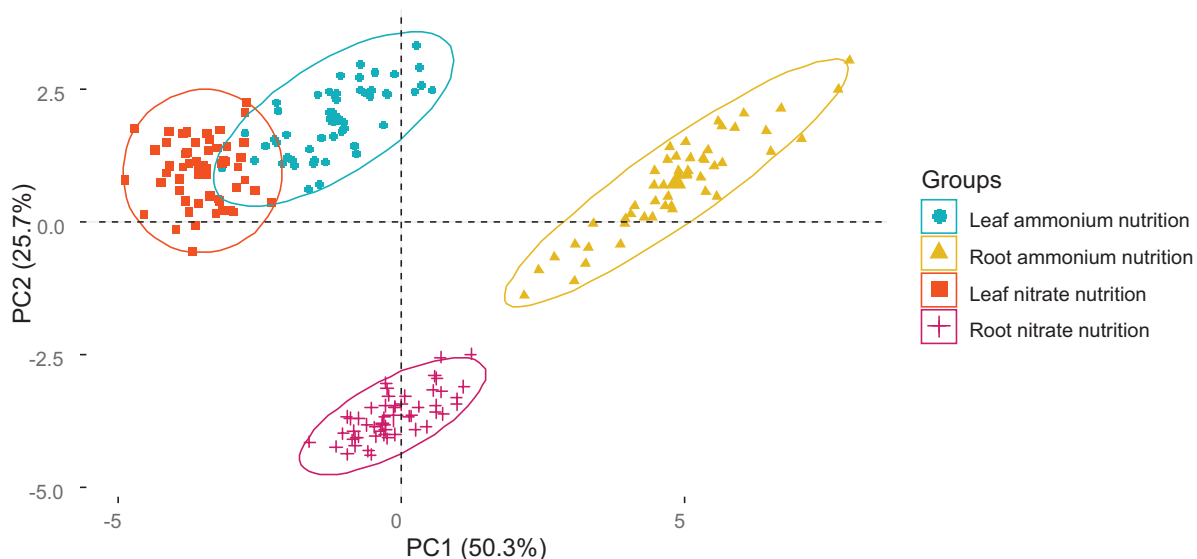


Fig. 3. Individual score plot of principal component analysis (PCA) for 52 accessions of *Brachypodium distachyon* grown under ammonium and nitrate nutrition, based on 20 metabolic traits determined in both leaf and root tissue. The variable score plot is shown in [Supplementary Fig. S2](#).

In this regard, the activity of TCA and anaplerotic enzymes is generally higher when plants are grown under ammonium nutrition (Vega-Mas *et al.*, 2019a; González-Moro *et al.*, 2021). Indeed, the amino acid accumulation commonly observed under ammonium nutrition is generally accompanied by organic acid depletion, notably in the leaves (Vega-Mas *et al.*, 2019a; Poucet *et al.*, 2021). Our data indicated that malate and citrate levels were very low in *B. distachyon* plants grown under NH_4^+ nutrition, and a general induction of the determined enzyme activities was observed, notably in the root (Supplementary Figs S5, S6). Regarding soluble carbohydrates, glucose content also tended to be lower under NH_4^+ nutrition, while fructose and sucrose were similar under both nutritional conditions (Supplementary Figs S5, S6). Another classical marker of NH_4^+ nutrition is the induction of GDH activity in the root (Cruz *et al.*, 2011; Sarasketa *et al.*, 2014). Accordingly, root GDH activity was higher in every accession studied, with a mean fold increase of ~ 2.5 (Supplementary Fig. S6R). Altogether, the general metabolic responses in our experiment were similar to those previously reported for Bd21 in De la Peña *et al.* (2019), wheat (Setián *et al.*, 2013), and rice (Kusano *et al.*, 2011), suggesting that the stimulation of NH_4^+ assimilation supported by TCA cycle functioning, notably in the root, to prevent photosynthetic damage is a general feature in grasses (De la Peña *et al.*, 2019). An increase in reactive oxygen species (ROS) production has been reported under NH_4^+ nutrition, often accompanied by an increase in cell antioxidant machinery in order to avoid or delay the occurrence of oxidative stress (Podgórska *et al.*, 2013; Y. Liu *et al.*, 2022). Concordantly, our analysis showed that total glutathione content was overall higher under NH_4^+ nutrition, notably in the roots (Supplementary Figs S5M, S6K). Importantly, most metabolic variables were influenced by the genotype, as indicated by the significant N source \times accession interaction observed with two-way ANOVA.

To further explore the obtained metabolic data, we performed HCA on heat map visualization of the whole dataset (Supplementary Fig. S7) and separating the two nutritional conditions (Fig. 4 for ammonium and Supplementary Fig. S8 for nitrate). Similar to the PCA result, clustering of the whole dataset clearly separated four groups, corresponding to leaf and root tissue under both nutrition types (Supplementary Fig. S7). When looking at the data under NH_4^+ nutrition, two main accession clusters were differentiated (Fig. 4). The cluster placed in the lower part of the heat map is formed by 18 accessions while the upper cluster is formed by 34 accessions. Among others, the differentiation of these two clusters was based on a lower sugar accumulation in the accessions placed in the lower cluster. Interestingly, when we searched for the top 10 NH_4^+ -sensitive and -tolerant accessions, as defined with the biomass ratio in Fig. 2B, a noteworthy pattern emerged. Most sensitive accessions clustered in the lower group, while the top 10 tolerant accessions clustered in the upper group (Fig. 4). Importantly, when examining the distribution of these

accessions in the heat maps performed with NO_3^- nutrition data, we found a more dispersed pattern with no clear separation of accessions (Supplementary Fig. S8). Taken together, our results indicate that the metabolic adaptation to NH_4^+ nutrition is a leading force to determine the intraspecific NH_4^+ sensitivity in *B. distachyon* using the NH_4^+ versus NO_3^- biomass ratio as the tolerance marker.

To identify the key explanatory metabolic variables associated with tolerance and sensitivity to NH_4^+ stress, we conducted PCA and OPLS-DA on the 20 metabolic variables derived from the selected top NH_4^+ -tolerant and -sensitive accessions, strengthened by the hierarchical clustering in Fig. 4. For this analysis, we excluded the two sensitive accessions located in the opposite cluster (Bd3-1 and RON2). To avoid a bias in the analysis because of the different size of the groups, two of the tolerant accessions (Mig3 and Koz1) were excluded. When the analysis was performed with the metabolic variables measured under NH_4^+ nutrition, sensitive and tolerant accessions were clearly segregated along PC1 and PC2 (Fig. 5A). Notably, the sensitive accessions exhibited a greater dispersion, while the tolerant ones displayed a narrower scattering. Likewise, the OPLS-DA model revealed increased variability among the most sensitive accessions compared with the tolerant accessions (Fig. 5B). To elucidate the most relevant metabolic variables, we derived VIP (variable importance in projection) values from the OPLS-DA model using a threshold of one. From the 14 significant variables, root and leaf sucrose and amino acid content, leaf NH_4^+ and starch content, and root PEPC and PK activity were positively associated with NH_4^+ tolerance (Fig. 5C). In contrast, leaf PEPC, PK, ICDH, and CS activity and root and leaf GDH activity were negatively associated with NH_4^+ tolerance (Fig. 5C). It was not possible to build the OPLS-DA model with the data obtained for these 16 accessions under nitrate conditions due to the lack of statistical significance in the first predictive component.

GWAS revealed gene loci potentially involved in *B. distachyon* tolerance to ammonium nutrition

To identify genetic loci potentially associated with *B. distachyon* tolerance upon NH_4^+ stress, we performed GWAS using the available dataset of dense SNPs specific to this genotype collection (Gordon *et al.*, 2017). We performed GWAS for a total of 91 traits, setting the significance threshold at $-\log_{10} P\text{-value} = 5$ (Supplementary Figs S9–S11). All significant SNPs are shown in Supplementary Table S6. Given the extensive amount of information obtained and considering that accession clustering revealed that the metabolic variation under NH_4^+ nutrition (Fig. 4), but not under nitric nutrition (Supplementary Fig. S8), was able to differentiate between NH_4^+ -sensitive and -tolerant accessions, we focused on the GWAS results associated with NH_4^+ nutrition. In particular, we focused on phenotypic traits such as biomass, glutathione content, and the significant variables derived from OPLS-DA.

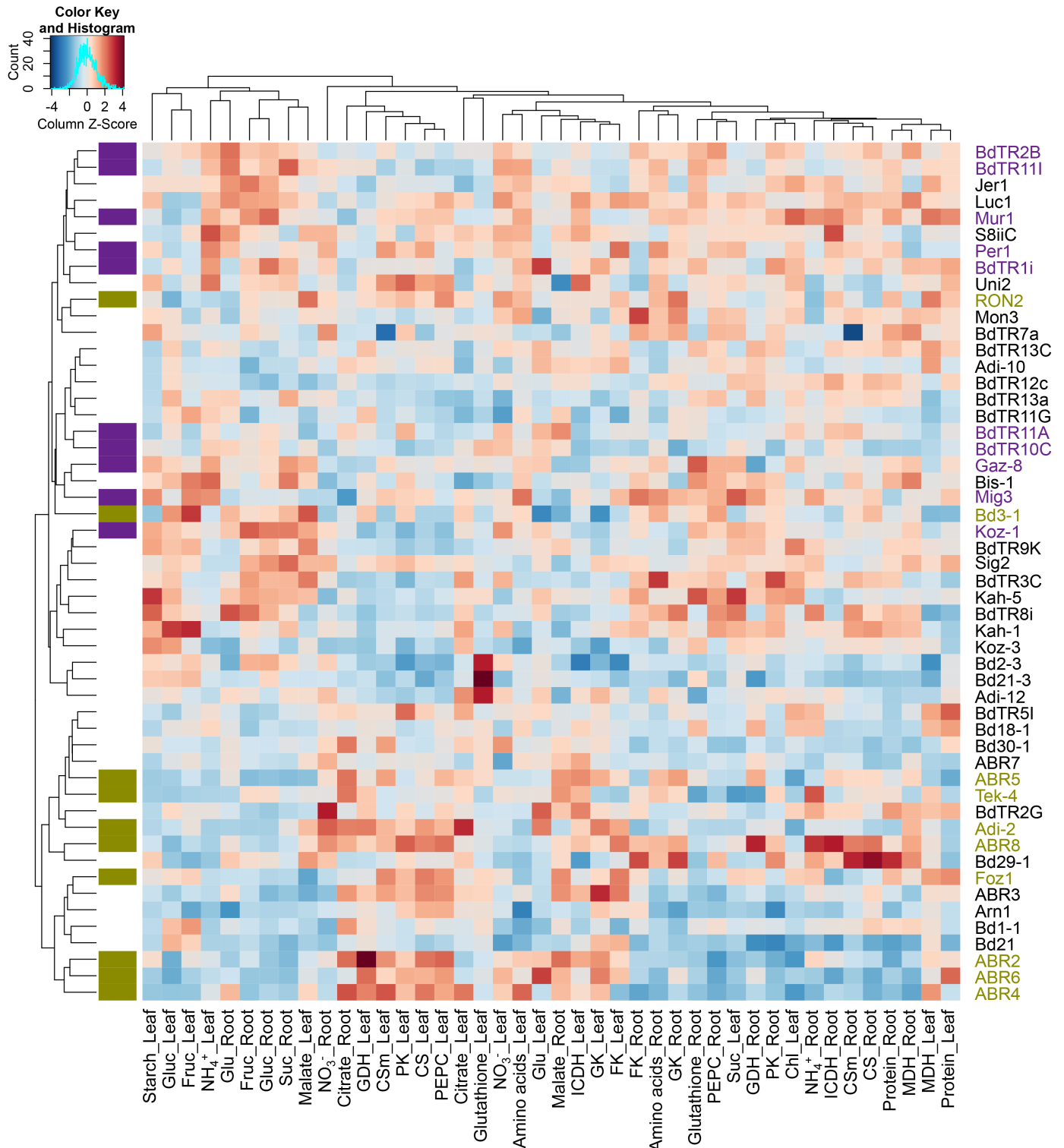


Fig. 4. Heat map visualization including hierarchical clustering for metabolites and enzymatic activities determined in leaf and root of 52 *B. distachyon* accessions grown under NH₄⁺ nutrition. Chl, chlorophyll; CS, citrate synthase; CSm, mitochondrial citrate synthase; FK, fructokinase; GDH, NAD-dependent glutamate dehydrogenase; GK, glucokinase; Glu, glutamate; ICDH, NADP-dependent isocitrate dehydrogenase; MDH, malate dehydrogenase; PEPC, phosphoenolpyruvate carboxylase; and PK, pyruvate kinase. The 10 accessions displaying the highest tolerance and the highest sensitivity to ammonium nutrition, as defined in Fig. 2, are shown in purple and dark green, respectively.

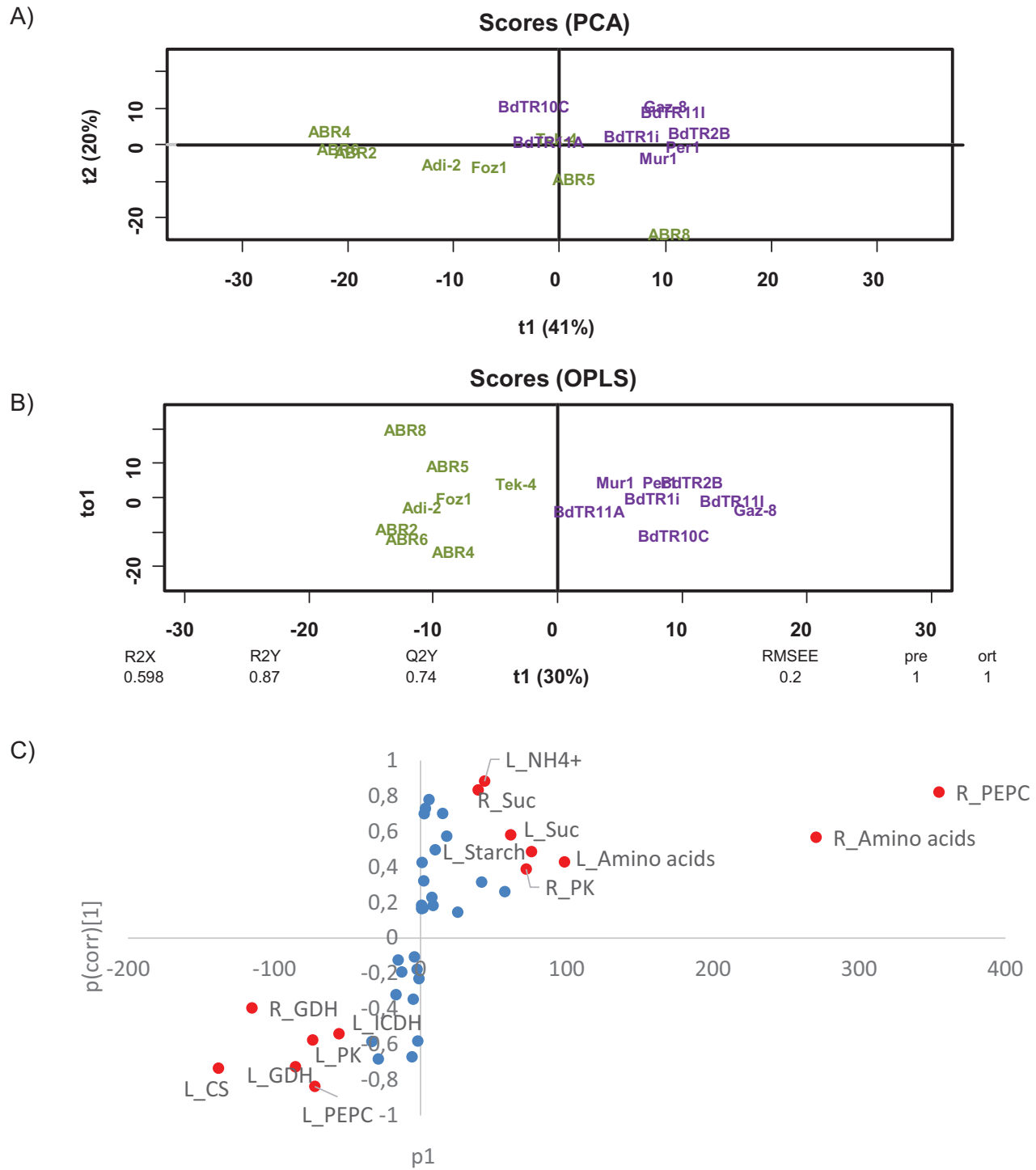


Fig. 5. Multivariate analyses. Principal component analysis (PCA) (A), orthogonal projection to latent structures-discriminant analysis (OPLS-DA) of correlation scaled scores (B), and S-plot of metabolic traits (C) performed with eight NH₄⁺-sensitive and -tolerant *Brachypodium distachyon* accessions under ammonium nutrition. In (A) and (B), dark green and purple refer to ammonium-sensitive and -tolerant accessions, respectively. Significant variables in (C) are indicated with red color.

For the significantly associated SNPs corresponding to these variables, we performed LD analysis and searched the loci present in the confidence regions surrounding those SNPs (Supplementary Table S7). To discuss potential candidate

genes among those present in the LD regions, we looked for available literature and also at their expression profile in the root of Bd21, as shown in Supplementary Table S8 (extracted from Supplementary Table S2).

For shoot, root, or whole-plant biomass under NH_4^+ nutrition, we did not find any SNP above the established threshold, probably as a consequence of the low number of accessions used for the study and the complexity of the biomass multigenic trait that may hinder the finding of significant SNPs. However, the analysis of the whole-plant biomass ratio (ammonium versus nitrate) revealed a significant SNP in chromosome 3 (ss.32878838 SNP, position 49357800). The genomic region associated with this SNP, following LD analysis, encompasses 16 genes (Supplementary Table S7). Two of the genes placed in the close vicinity of the significant SNPs, *Bradi3g48060* and *Bradi3g48070*, which code for a homolog of Arabidopsis CLAVATA2 (*CLV2*) and for a member of the abscisic acid (ABA)-responsive kinase substrates (AKS) basic helix-loop-helix (bHLH) transcription factor family, respectively, were induced in the root of Bd21 under ammonium nutrition (Supplementary Table S8). *CLV2* is a known leucine-rich repeat receptor-like protein involved in plant growth and development (Pan *et al.*, 2016). In Arabidopsis, AKS transcription factors facilitate ABA-dependent K^+ uptake and root elongation, among others through the regulation of the expression of the K^+ transporters *KAT1*, *KAT2*, and *AKT1* (Takahashi *et al.*, 2013; Tian *et al.*, 2015). NH_4^+ and K^+ compete for their uptake, and K^+ deficiency is among the causes that lead to NH_4^+ stress (Coletto *et al.*, 2023). Interestingly, several potassium transporters including *KAT2* (*Bradi2g06750*), *AKT1* (*Bradi2g45170*), and *AKT2* (*Bradi2g24450*) were differentially expressed in Bd21 root as a function of the N source provided (Supplementary Table S2). We looked for Arabidopsis AKS transcription factor orthologs in the *B. distachyon* reference genome and found three genes (*Bradi2g57800*, *Bradi3g39927*, and *Bradi3g48070*). We determined their expression in the ammonium-sensitive ABR2 and the ammonium-tolerant Koz-1 accessions, and observed that *Bradi2g57800* and *Bradi3g48070* were induced under ammonium nutrition only in Koz-1 (Supplementary Fig. S12A). We also determined *CLV2* expression, with no differences observed between genotypes (Supplementary Fig. S12B). Altogether, our results suggest that AKS transcription factors might be involved in NH_4^+ tolerance. Future studies, for instance with the use of mutants and/or overexpressing plants, are necessary to confirm the contribution of these genes to plant tolerance of NH_4^+ stress.

Root glutathione content correlates with *B. distachyon* tolerance to ammonium nutrition

ROS overproduction is often described in plants grown under NH_4^+ nutrition, considering the occurrence of oxidative stress as one of the causes of NH_4^+ stress. The origin of NH_4^+ -dependent ROS overproduction is linked to, among others, an increased mitochondrial electron transport chain activity (Rasmusson *et al.*, 2020), the non-consumption of photosynthetically generated reductants during NO_3^- reduction (Podgórska *et al.*, 2013), and the Fenton reaction due

to reactive Fe accumulation in the root (Y. Liu *et al.*, 2022). Thus, cell antioxidant capacity is often enhanced under NH_4^+ nutrition to buffer ROS production. Glutathione is a sulfur-containing compound that, together with ascorbate, is the main non-enzymatic antioxidant. Our transcriptomic analysis indicated 'glutathione metabolic process' as an important biological process associated with the genes induced upon ammonium nutrition (Fig. 1). This category contained 29 genes, which corresponded to 26 glutathione transferases, the two main enzymes in charge of glutathione synthesis, and one glutathione reductase (Supplementary Table S3). When we determined the total glutathione content in the assessed *B. distachyon* accessions, we observed that glutathione levels were generally higher under NH_4^+ nutrition, notably in the root (Supplementary Figs S5M, S6K). Although glutathione was not among the significant variables that emerged from OPLS-DA, root glutathione was the metabolic variable that showed the highest correlation with ammonium tolerance using the NH_4^+ versus NO_3^- biomass ratio as the tolerance definer ($R^2=0.48$; Supplementary Fig. S13C). Unfortunately, no SNP above the significance threshold was found for root GSH content (Supplementary Fig. S11K). In contrast, the GWAS detected nine significant SNPs associated with leaf glutathione content, with the SNP ss.31890199 of chromosome 3 showing a very high significance ($-\log_{10} P\text{-value}=12.26$) (Supplementary Fig. S10M; Supplementary Table S6). The region surrounding this SNP contained six loci, three of them showing significant differential expression in Bd1 roots as a function of the N source provided (Supplementary Table S8). These three genes correspond to a cyclin, a RING/FYVE/PHD-type zinc finger superfamily protein, and a pentatricopeptide repeat (PPR) family protein. However, there is no evidence of any link between these genes and glutathione content in plants.

BdGDH2 is associated with *B. distachyon* ammonium tolerance

GDH is a reversible enzyme that *in vitro* can both assimilate NH_4^+ to form glutamate and deaminate glutamate to form 2-oxoglutarate (2-OG). Although many efforts have been dedicated to elucidating the role of GDH *in vivo*, its reversible nature remains controversial. In general, evidence supports that GDH would be mainly operating in its deaminating role (Fontaine *et al.*, 2012). However, studies performed in tomato (Vega-Mas *et al.*, 2019b) and tobacco (Skopelitis *et al.*, 2006) with the use of GS/GOGAT inhibitors have shown that, under certain conditions, NH_4^+ can be incorporated into Glu and/or Gln even when GS/GOGAT is inhibited, thus supporting the GDH aminating role at least in these *Solanaceae* species. However, GDH does not seem to favor *in vivo* NH_4^+ assimilation in wheat (Vega-Mas *et al.*, 2019a). In *B. distachyon*, closely related to wheat, we could expect that the enhanced GDH activity reported in NH_4^+ -fed plants, mainly in the root (Fig. 6A; Supplementary Fig. S6R), could be acting in the

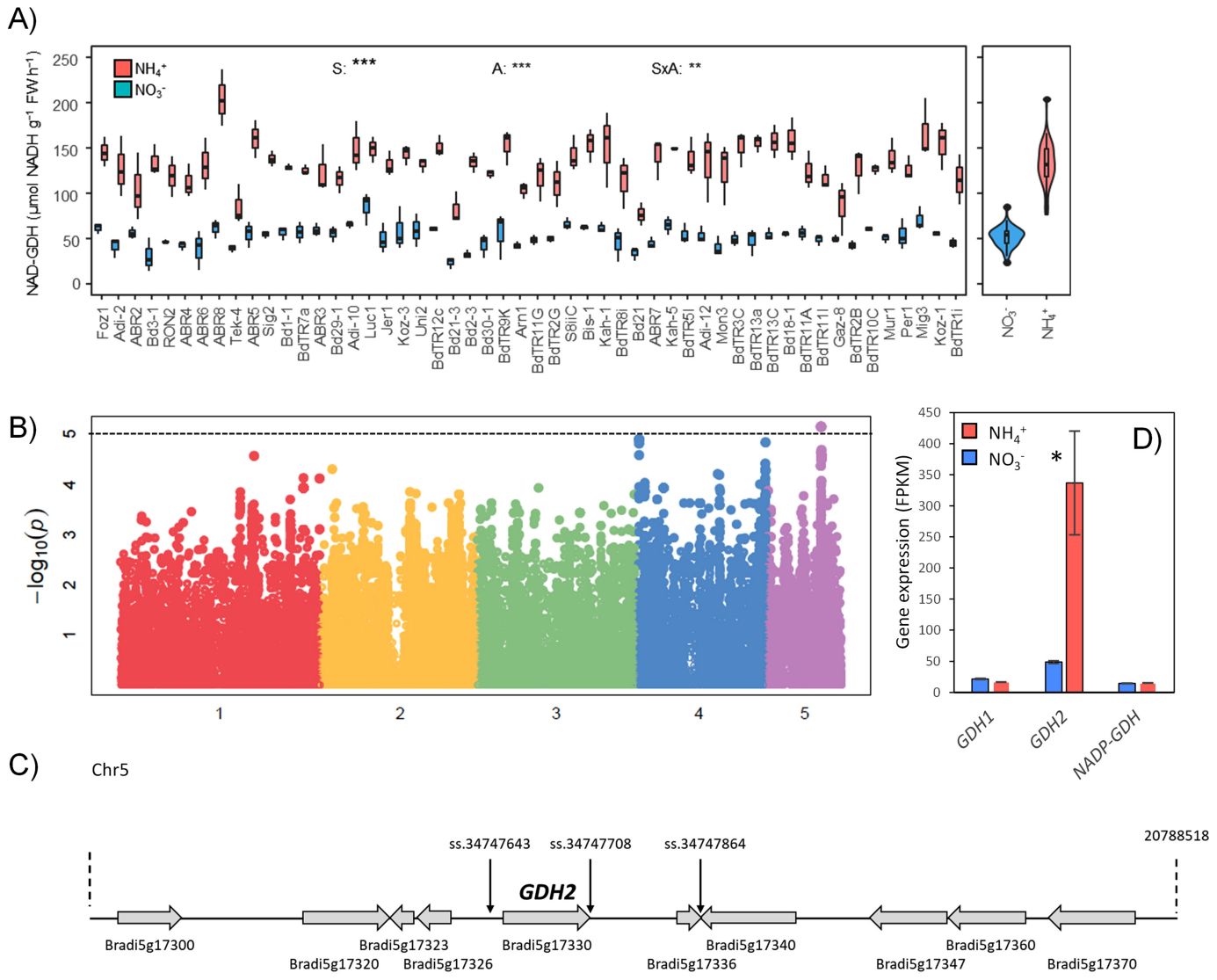


Fig. 6. Root glutamate dehydrogenase (GDH) activity of 52 accessions of *Brachypodium distachyon* grown under nitrate or ammonium as N source. Violin plots on the right side show the overall distribution of the trait (A). Manhattan plot of GWAS for root GDH activity of NH₄⁺-fed plants (B). Genetic map of the LD region corresponding to the three significant SNPs (ss.34747643, ss.34747708, and ss.34747864) found in chromosome 5 (C). GDH family gene expression pattern in roots of Bd21 plants grown with ammonium or nitrate as the exclusive source of nitrogen (D). Values represent the mean ±SE (n=3). Each biological replicate corresponds to the three or 12 plants grown in the same tank for (A) and (D), respectively. In (A), significant differences from two-way ANOVA are indicated (*P<0.05, **P<0.01, ***P<0.001) for N source effect (S) and accession (A), and their interaction (SxA). In (D), an asterisk (*) indicates a significant nitrogen source effect (t-test, P<0.05).

generation of 2-OG to limit the depletion of organic acids provoked by high NH₄⁺. Indeed, GDH activity was negatively correlated with the biomass ratio (Supplementary Fig. S13), and displayed a negative association with NH₄⁺ tolerance in OPLS-DA (Fig. 5C).

Interestingly, GWAS uncovered three significant SNPs in chromosome 5 (ss.34747643, ss.34747708, and ss.34747864) associated with root GDH activity (Fig. 6B). These three SNPs cover a genomic region of 10.57 kb where the gene that encodes the mitochondrial GDH enzyme (*GDH2*; *Bradi5g17330*) is located (Fig. 6C; Supplementary Table S7).

Indeed, in general, *GDH2* is the GDH isoform that experiences the highest induction upon ammonium nutrition (Sarasketa et al., 2016). Notably, the Bd21 transcriptome showed that *GDH2* was the isoform specifically induced in NH₄⁺-fed plants (Supplementary Table S2; Fig. 6D). We also determined *GDH2* expression in the root of two accessions with contrasting ammonium tolerance and reported a similar induction in ammonium-fed plants for both accessions (Supplementary Fig. S12C). Altogether, OPLS-DA followed by GWAS indicate that the *BdGDH2* gene is associated with *B. distachyon* natural variation upon ammonium nutrition. In addition, finding

the *BdGDH2* gene associated with GDH activity reveals the power of GWAS even with a small panel of accessions when robust phenotyping is performed.

Phosphoenolpyruvate carboxylase as a target to improve ammonium tolerance in grasses

OPLS-DA indicated a pivotal role for PEPC activity, particularly in the root, as the most crucial enzymatic activity for discriminating among the NH_4^+ -sensitive and -tolerant accessions (Fig. 5C). PEPC catalyzes the carboxylation of phosphoenolpyruvate (PEP) to oxaloacetate (OAA) using HCO_3^- and inorganic phosphate. In C_3 plants, one of the fundamental functions of PEPC is to anaplerotically replenish TCA cycle intermediates, notably when intermediates of the cycle are removed to maintain different biosynthetic pathways, as in the case of NH_4^+ nutrition (Lasa *et al.*, 2002; Vega-Mas *et al.*, 2019a; González-Moro *et al.*, 2021). Indeed, studies with Arabidopsis mutants demonstrated that malate provision partially depends on PEPC activity (Shi *et al.*, 2015; Feria *et al.*, 2016). Recently, RNAi sorghum lines that display a decreased expression of the main root PEPC isoform (*SbPPC3*) and reduced root PEPC activity displayed NH_4^+ hypersensitivity, meaning lower biomass accumulation in transgenic plants with respect to wild-type plants. In addition, the silenced plants presented higher NH_4^+ accumulation in the root and the alteration of normal TCA functioning (Marín-Peña *et al.*, 2024). PK was also induced in NH_4^+ -fed plants and associated with NH_4^+ tolerance in a similar way to PEPC (Fig. 5C; Supplementary Figs S5, S6). PK uses PEP to provide pyruvate to the TCA cycle and its activity is regulated by the cellular demand for C skeletons for NH_4^+ assimilation (Baysdorfer and Bassham, 1984). In tomato leaves, the conjoint action of PK and PEPC was also proposed as central to ensure carbon flux for energy production under ammonium nutrition (Poucet *et al.*, 2022). Therefore, PEP seems to be a crucial checkpoint in the capacity of the root cell to maintain NH_4^+ assimilation, and PK and PEPC are in charge of channeling the PEP pool towards pyruvate or OAA, respectively. Another important function of non-photosynthetic PEPC is linked to the regulation of cell pH homeostasis, through the so-called biochemical pH-stat that consists of carboxylation and decarboxylation reactions that produce and consume protons (Feng *et al.*, 2020). Interestingly, OPLS-DA showed that root PEPC was positively associated with ammonium tolerance, while leaf PEPC showed an opposite association (Fig. 5C). Indeed, leaf PEPC activity was the variable that displayed the highest negative correlation with the $\text{NH}_4^+/\text{NO}_3^-$ biomass ratio (Supplementary Fig. S13A). Therefore, the induction of the TCA cycle to provide C skeletons in the root can be interpreted as a positive trait for NH_4^+ tolerance, while the induction in the leaf can be considered as a negative trait. In this regard, Arabidopsis plants impaired in proper root Gln synthesis are sensitive towards NH_4^+ stress (Guan *et al.*, 2016), while plants that prevent Gln accumulation in leaves are more

tolerant (Hachiya *et al.*, 2021; Xie *et al.*, 2023). Thus, in consonance with previous studies, our data support the idea that a high root NH_4^+ assimilation capacity would be beneficial for the plant, while the high assimilation in leaves would be detrimental for NH_4^+ tolerance.

GWAS for root PEPC activity showed a unique significant SNP (CHR2_ss.31408046; $-\log_{10}$ P-value 5.26; Supplementary Table S6). LD analysis indicated eight loci in the genomic region associated with this SNP (Supplementary Table S7). Five of these loci are genes that encode proteins with a domain corresponding to protease inhibitors annotated as 'Potato inhibitor I family' that are potentially related to pathogen resistance (Supplementary Table S7). Two of these genes (*Bradi2g39260* and *Bradi2g39280*) showed higher expression in ammonium-fed Bd21 roots (Supplementary Table S2). However, there is no obvious link between this class of proteins and PEPC activity or NH_4^+ nutrition. Interestingly, the GWAS performed with leaf PEPC activity showed 10 significant SNPs in chromosome 2 within a genomic region of 18 kb (top SNP CHR2_ss.31624104, $-\log_{10}$ P-value 6.17; Supplementary Table S6). Importantly, the genomic region linked to these SNPs (Supplementary Table S7) comprises two genes coding for NADP⁺-dependent malic enzyme (ME; *Bradi2g49542* and *Bradi2g49532*). The joint action of PEPC and ME is considered as a metabolic rectifier of cytosolic pH perturbations, and thus is central for the functioning of the biochemical pH-stat model (Davies, 1973; Sakano, 2001). This model has been used to explain organic acid depletion under ammonium nutrition (Pasqualini *et al.*, 2001; Poucet *et al.*, 2021). Altogether, our data suggest that in *B. distachyon* the higher activity of PEPC would be related to TCA replenishment rather than to the control of cytosolic pH and that ME activity might be a determinant for leaf PEPC activity.

Conclusion

In this work, we used the non-domesticated grass model *B. distachyon* to advance our understanding of the metabolic and genetic basis of NH_4^+ tolerance. We carried out a transcriptomic analysis in the root of the Bd21 accession and conducted a natural variation study determining key metabolic traits associated with NH_4^+ tolerance in the roots and leaves of 52 accessions. We evidenced that *B. distachyon* displays extensive variability towards NH_4^+ tolerance and that the root metabolic adaptation to NH_4^+ nutrition is essential for the plant to cope with NH_4^+ stress. Multivariate analysis revealed that NH_4^+ assimilation in the root and PEPC activity have a major effect on determining an accession's tolerance or sensitivity towards NH_4^+ nutrition. Additionally, taking advantage of available genetic information of the selected accession, we performed GWAS for all the variables analyzed and report several loci associated with *B. distachyon* growth and metabolic adaptation to ammonium nutrition. Among others, we suggest that AKS transcription factors might be associated with ammonium tolerance. In addition, we

found that the *GDH2* gene was associated with the induction of root GDH activity observed under NH_4^+ nutrition. Importantly, according to our multivariate analysis, GDH induction was negatively associated with NH_4^+ tolerance. In addition, two genes encoding ME were associated with leaf PEPC activity. These results highlight the importance of the coordination between the different players associated with the TCA cycle, in particular the nexus between C_3 and C_4 organic acids, and emphasize the importance of C management under NH_4^+ nutrition. Altogether, our work underlines that primary metabolism is a key definer of *B. distachyon* NH_4^+ tolerance and evidences the utility of *B. distachyon* as a model of N nutrition in crop grasses. Improving crop NUE, and ammonium use efficiency in particular, is of great interest to mitigate the environmental contamination associated with N fertilization in order to attain a more sustainable agriculture. In this work, we revealed cell metabolism as a determinant of the natural variation to ammonium tolerance. The identification and future validation of the genetic basis associated with the control of the metabolic adaptation to ammonium nutrition will be of great importance in the search for crop genotypes better adapted to this nutrition and will contribute to reduce the N losses in agricultural systems.

Supplementary data

The following supplementary data are available at [JXB online](#).

Table S1. Primers used for qPCR gene expression analysis.

Table S2. Differentially expressed genes in roots of *Brachypodium distachyon* Bd21.

Table S3. Full list of enriched GO functional classes.

Table S4. Expression of *Brachypodium distachyon* Bd21 *NRT1;1*, *NRT2*, and *AMT1* genes.

Table S5. Full dataset generated in this study.

Table S6. Significant SNPs revealed after genome-wide association analysis for all the variables determined.

Table S7. Loci associated with selected variables.

Table S8. Expression of loci associated with the selected variables as indicated in [Supplementary Table S7](#) in *B. distachyon* Bd21.

Fig. S1. Heat map of pairwise kinship values and plot of the first two principal components.

Fig. S2. Image of *B. distachyon* Bd21 grown under ammonium or nitrate nutrition.

Fig. S3. Natural variation in shoot and root biomass.

Fig. S4. Bidimensional PCA plot of variables plot performed with the whole dataset generated in this study.

Fig. S5. Natural variation in leaf metabolite content and enzyme activities.

Fig. S6. Natural variation in root metabolite content and enzyme activities.

Fig. S7. Heat map visualization including hierarchical clustering for metabolites and enzymatic activities determined in leaf and root under NO_3^- and NH_4^+ nutrition.

Fig. S8. Heat map visualization including hierarchical clustering for metabolites and enzymatic activities determined in leaf and root under NO_3^- nutrition.

Fig. S9. Natural genetic variation for plant growth.

Fig. S10. Natural genetic variation for leaf metabolic traits and enzyme activities.

Fig. S11. Natural genetic variation for root metabolic traits and enzyme activities.

Fig. S12. Gene expression (qPCR) of *AKS* transcription factors and *CLV2* in the root of ammonium-sensitive (*ABR2*) and ammonium-tolerant (*Koz-1*) accessions grown under exclusive NH_4^+ or NO_3^- supply.

Fig. S13. Correlation matrixes for all measured traits in leaf and root.

Acknowledgements

We would like to thank Dr Ludmila Tyler (University of Massachusetts Amherst, USA), Dr Amy Cartwright (DOE Joint Genome Institute, USA), Dr Luis Alejandro Mur, and John Doonan (Aberystwyth University, UK) for kindly providing us with seeds of the *B. distachyon* accessions used in this study. We would like to thank Dr John Vogel (DOE Joint Genome Institute, USA) for facilitating genomic data and Dr Bruno Contreras-Moreira for his assistance in preparing the vcf file for GWAS analysis. The authors also thank SGIker (UPV/EHU, ERDF, UE) for the technical and human support provided.

Author contributions

DM: conceived the project and designed the experiment; DM and MBGM: supervised the work; PC, MBGM, and YG: supported the experimental design; EI and FM: supported the GWAS and performed LD analysis; MdLP and IVM: grew plants and performed biomass measurements; YG: facilitated access to the metabolic phenotyping platform; MdLP, CC, and TP: performed metabolic analysis; LU and JAUG: performed gene expression analysis; MdLP and DM: data analysis and wrote the article. All authors edited and approved the final manuscript.

Conflict of interest

The authors declare no competing interests.

Funding

This work was supported by the Consolidated Groups program (IT1560-22) of the Basque Government, by MICIN/AEI/10.13039/501100011033 (project PID2020-113385RBI00) co-funded by 'ERDF A way of making Europe'. High-throughput metabolic assays were funded by the Horizon 2020 European Plant Phenotyping Network Transnational Access Program (EPPN2020 grant agreement no. 731013) and by PHENOME (ANR-11-INBS-0012). MdLP held a doctoral scholarship (Conv. 672) associated with COLCIENCIAS (Department of Science, Technology and Innovation of Colombia) and the Department of Magdalena. TP

benefited from a PhD from the University of the Basque Country (UPV/EHU, Spain).

Data availability

All data supporting the findings of this study are available within the paper and its supplementary data. Raw sequencing data generated in this study are available in the Gene Expression Omnibus (GEO) database under accession GSE275962.

References

- Anders S, Pyl PT, Huber W. 2015. HTSeq—a Python framework to work with high-throughput sequencing data. *Bioinformatics* **31**, 166–169.
- Anoop VM, Basu U, McCammon MT, McAlister-Henn L, Taylor GJ. 2003. Modulation of citrate metabolism alters aluminum tolerance in yeast and transgenic canola overexpressing a mitochondrial citrate synthase. *Plant Physiology* **132**, 2205–2217.
- Ariz I, Cruz C, Moran JF, Gonzalez-Moro MB, García-Olaverri C, González-Murua C, Martins-Loução MA, Aparicio-Tejo PM. 2011. Depletion of the heaviest stable N isotope is associated with $\text{NH}_4^+/\text{NH}_3$ toxicity in NH_4^+ -fed plants. *BMC Plant Biology* **11**, 83.
- Bantan-Polak T, Kassai M, Grant KB. 2001. A comparison of fluorescamine and naphthalene-2,3-dicarboxaldehyde fluorogenic reagents for microplate-based detection of amino acids. *Analytical Biochemistry* **297**, 128–136.
- Baysdorfer C, Bassham JA. 1984. Spinach pyruvate kinase isoforms: partial purification and regulatory properties. *Plant Physiology* **74**, 374–379.
- Bénard C, Gibon Y. 2016. Measurement of enzyme activities and optimization of continuous and discontinuous assays. *Current Protocols in Plant Biology* **1**, 247–262.
- Breseghele F, Sorrells ME. 2006. Association mapping for kernel size and milling quality in wheat (*Triticum aestivum* L.) cultivars. *Genetics* **172**, 1165–1177.
- Britto DT, Kronzucker HJ. 2002. NH_4^+ toxicity in higher plants: a critical review. *Journal of Plant Physiology* **159**, 567–584.
- Britto DT, Kronzucker HJ. 2013. Ecological significance and complexity of N-source preference in plants. *Annals of Botany* **112**, 957–963.
- Catalan P, López-Álvarez D, Díaz-Pérez A, Sancho R, López-Herránz ML. 2016. Phylogeny and evolution of the genus *Brachypodium*. In: Vogel J, ed. *Genetics and genomics of Brachypodium*. Plant Genetics and Genomics: Crops and Models, vol 18. Cham: Springer, 9–38.
- Chen H, Zhang Q, Wang X, Zhang J, Ismail AM, Zhang Z. 2021. Nitrogen form-mediated ethylene signal regulates root-to-shoot K^+ translocation via NRT1.5. *Plant, Cell & Environment* **44**, 3806–3818.
- Coletto I, Marín-Peña A, Urbano-Gámez JA, González-Hernández AI, Shi W, Li G, Marino D. 2023. Nutrients interact: the case of ammonium nutrition and essential mineral cations. *Journal of Experimental Botany* **74**, 6131–6144.
- Coskun D, Britto DT, Shi W, Kronzucker HJ. 2017. Nitrogen transformations in modern agriculture and the role of biological nitrification inhibition. *Nature Plants* **3**, 17074.
- Cruz C, Domínguez-Valdivia MD, Aparicio-Tejo PM, Lamsfus C, Bio A, Martins-Loução MA, Moran JF. 2011. Intra-specific variation in pea responses to ammonium nutrition leads to different degrees of tolerance. *Environmental and Experimental Botany* **70**, 233–243.
- David LC, Girin T, Fleurisson E, Phommabouth E, Mahfoudhi A, Citerne S, Berquin P, Daniel-Vedele F, Krapp A, Ferrario-Méry S. 2019. Developmental and physiological responses of *Brachypodium distachyon* to fluctuating nitrogen availability. *Scientific Reports* **9**, 3824.
- Davies DD. 1973. Control of and by pH. *Symposia of the Society for Experimental Biology* **27**, 513–529.
- De la Peña M, González-Moro MB, Marino D. 2019. Providing carbon skeletons to sustain amide synthesis in roots underlines the suitability of *Brachypodium distachyon* for the study of ammonium stress in cereals. *AoB Plants* **11**, plz029.
- De la Peña M, Marín-Peña AJ, Urmeneta L, Coletto I, Castillo-González J, van Liempd SM, Falcón-Pérez JM, Álvarez-Fernández A, González-Moro MB, Marino D. 2022. Ammonium nutrition interacts with iron homeostasis in *Brachypodium distachyon*. *Journal of Experimental Botany* **73**, 263–274.
- De la Peña M, Ruiz-Romero R, Romero HM. 2023. Nitrogen use efficiency in oil palm seedlings: unravelling the untapped potential of elevated external ammonium supply. *Plants (Basel, Switzerland)* **12**, 2819.
- Di D-W, Sun L, Zhang X, Li G, Kronzucker HJ, Shi W. 2018. Involvement of auxin in the regulation of ammonium tolerance in rice (*Oryza sativa* L.). *Plant and Soil* **432**, 373–387.
- Esteban R, Ariz I, Cruz C, Moran JF. 2016. Review: mechanism of ammonium toxicity and the quest for tolerance. *Plant Science* **248**, 92–101.
- Feng H, Fan X, Miller AJ, Xu G. 2020. Plant nitrogen uptake and assimilation: regulation of cellular pH homeostasis. *Journal of Experimental Botany* **71**, 4380–4392.
- Feria AB, Bosch N, Sánchez A, Nieto-Ingelmo AI, de la Osa C, Echevarría C, García-Mauriño S, Monreal JA. 2016. Phosphoenolpyruvate carboxylase (PEPC) and PEPC-kinase (PEPC-k) isoenzymes in *Arabidopsis thaliana*: role in control and abiotic stress conditions. *Planta* **244**, 901–913.
- Fontaine JX, Terce-Laforgue T, Armengaud P, et al. 2012. Characterization of a NADH-dependent glutamate dehydrogenase mutant of *Arabidopsis* demonstrates the key role of this enzyme in root carbon and nitrogen metabolism. *The Plant Cell* **24**, 4044–4065.
- Gibon Y, Blaessing OE, Hannemann J, Carillo P, Höhne M, Hendriks JHM, Palacios N, Cross J, Selbig J, Stitt M. 2004. A robot-based platform to measure multiple enzyme activities in *Arabidopsis* using a set of cycling assays: comparison of changes of enzyme activities and transcript levels during diurnal cycles and in prolonged darkness. *The Plant Cell* **16**, 3304–3325.
- Girin T, David LC, Chardin C, Sibout R, Krapp A, Ferrario-Méry S, Daniel-Vedele F. 2014. *Brachypodium*: a promising hub between model species and cereals. *Journal of Experimental Botany* **65**, 5683–5696.
- Glazowska S, Baldwin L, Mravec J, Bukh C, Fangel JU, Willats WGT, Schjoerring JK. 2019. The source of inorganic nitrogen has distinct effects on cell wall composition in *Brachypodium distachyon*. *Journal of Experimental Botany* **70**, 6461–6473.
- González-Moro MB, González-Moro I, de la Peña M, Estavillo JM, Aparicio-Tejo PM, Marino D, González-Murua C, Vega-Mas I. 2021. A multi-species analysis defines anaplerotic enzymes and amides as metabolic markers for ammonium nutrition. *Frontiers in Plant Science* **11**, 632285.
- Goodstein DM, Shu S, Howson R, et al. 2012. Phytozome: a comparative platform for green plant genomics. *Nucleic Acids Research* **40**, D1178–D1186.
- Gordon SP, Contreras-Moreira B, Woods DP, et al. 2017. Extensive gene content variation in the *Brachypodium distachyon* pan-genome correlates with population structure. *Nature Communications* **8**, 2184.
- Griffith OW. 1980. Determination of glutathione and glutathione disulfide using glutathione reductase and 2-vinylpyridine. *Analytical Biochemistry* **106**, 207–212.
- Guan M, De Bang TC, Pedersen C, Schjoerring JK. 2016. Cytosolic glutamine synthetase Gln1;2 is the main isozyme contributing to GS1 activity and can be up-regulated to relieve ammonium toxicity. *Plant Physiology* **171**, 1921–1933.
- Hachiya T, Inaba J, Wakazaki M, et al. 2021. Excessive ammonium assimilation by plastidic glutamine synthetase causes ammonium toxicity in *Arabidopsis thaliana*. *Nature Communications* **12**, 4944.
- Hasterok R, Catalan P, Hazen SP, Roulin AC, Vogel JP, Wang K, Mur LAJ. 2022. *Brachypodium*: 20 years as a grass biology model system; the way forward? *Trends in Plant Science* **27**, 1002–1016.

- Hessini K, Hamed KB, Gandour M, Mejri M, Abdelly C, Cruz C. 2013. Ammonium nutrition in the halophyte *Spartina alterniflora* under salt stress: evidence for a priming effect of ammonium? *Plant and Soil* **370**, 163–173.
- Katz E, Knapp A, Lensink M, Keller CK, Stefani J, Li J-J, Shane E, Tuermer-Lee K, Bloom AJ, Kliebenstein DJ. 2022. Genetic variation underlying differential ammonium and nitrate responses in *Arabidopsis thaliana*. *The Plant Cell* **34**, 4696–4713.
- Kellog EA. 2015. *Brachypodium distachyon* as a genetic model system. *Annual Review of Genetics* **49**, 1–20.
- Kim D, Paggi JM, Park C, Bennett C, Salzberg SL. 2019. Graph-based genome alignment and genotyping with HISAT2 and HISAT-genotype. *Nature Biotechnology* **37**, 907–915.
- Kolberg L, Raudvere U, Kuzmin I, Adler P, Vilo J, Peterson H. 2023. g:Profiler—interoperable web service for functional enrichment analysis and gene identifier mapping (2023 update). *Nucleic Acids Research* **51**, W207–W212.
- Kong L, Zhang Y, Zhang B, Li H, Wang Z, Si J, Fan S, Feng B. 2022. Does energy cost constitute the primary cause of ammonium toxicity in plants? *Planta* **256**, 62.
- Kusano M, Tabuchi M, Fukushima A, *et al.* 2011. Metabolomics data reveal a crucial role of cytosolic glutamine synthetase 1;1 in coordinating metabolic balance in rice. *The Plant Journal* **66**, 456–466.
- Lasa B, Frechilla S, Aparicio-Tejo PM, Lamsfus C. 2002. Role of glutamate dehydrogenase and phosphoenolpyruvate carboxylase activity in ammonium nutrition tolerance in roots. *Plant Physiology and Biochemistry* **40**, 969–976.
- Lassaletta L, Billen G, Garnier J, Bouwman L, Velazquez E, Mueller ND, Gerber JS. 2016. Nitrogen use in the global food system: past trends and future trajectories of agronomic performance, pollution, trade, and dietary demand. *Environmental Research Letters* **11**, 095007.
- Lê S, Josse J, Husson F. 2008. FactoMineR: an R package for multivariate analysis. *Journal of Statistical Software* **25**, 1–18.
- Lenth R, Singmann H, Love J, Buerkner P, Herve M. 2018. Package 'Emmeans'. R Package Version 4.0-3. <http://cran.r-project.org/package=emmeans>
- Liu XX, Zhang HH, Zhu QY, *et al.* 2022. Phloem iron remodels root development in response to ammonium as the major nitrogen source. *Nature Communications* **13**, 561.
- Liu Y, Maniero RA, Giehl RFH, Melzer M, Steensma P, Krouk G, Fitzpatrick TB, von Wirén N. 2022. PDX1.1-dependent biosynthesis of vitamin B6 protects roots from ammonium-induced oxidative stress. *Molecular Plant* **15**, 820–839.
- Love MI, Huber W, Anders S. 2014. Moderated estimation of fold change and dispersion for RNA-seq data with DESeq2. *Genome Biology* **15**, 550.
- Mangin B, Siberchicot A, Nicolas S, Doligez A, This P, Cierco-Ayrolles C. 2012. Novel measures of linkage disequilibrium that correct the bias due to population structure and relatedness. *Heredity* **108**, 285–291.
- Marín-Peña AJ, Vega-Mas I, Busturia I, de la Osa C, González-Moro MB, Monreal JA, Marino D. 2024. Root phosphoenolpyruvate carboxylase activity is essential for *Sorghum bicolor* tolerance to ammonium nutrition. *Plant Physiology and Biochemistry* **206**, 108312.
- Pan L, Lv S, Yang N, Lv Y, Liu Z, Wu J, Wang G. 2016. The multifunction of CLAVATA2 in plant development and immunity. *Frontiers in Plant Science* **7**, 1573.
- Pasqualini S, Ederli L, Piccioni C, Batini P, Bellucci M, Arcioni S, Antonielli M. 2001. Metabolic regulation and gene expression of root phosphoenolpyruvate carboxylase by different nitrogen sources. *Plant, Cell & Environment* **24**, 439–447.
- Plett D, Toubia J, Garnett T, Tester M, Kaiser BN, Baumann U. 2010. Dichotomy in the NRT gene families of dicots and grass species. *PLoS One* **5**, e15289.
- Podgórska A, Gieczewska K, Łukawska-Kuźma K, Rasmusson AG, Gardeström P, Szal B. 2013. Long-term ammonium nutrition of *Arabidopsis* increases the extrachloroplastic NAD(P)H/NAD(P)⁺ ratio and mitochondrial reactive oxygen species level in leaves but does not impair photosynthetic capacity. *Plant, Cell & Environment* **36**, 2034–2045.
- Poucet T, Beauvoit B, Gonzalez-Moro MB, Cabasson C, Pétriacoq P, Flandin A, Gibon Y, Marino D, Dieuaide-Noubhani M. 2022. Impaired cell growth under ammonium stress explained by modeling the energy cost of vacuole expansion in tomato leaves. *The Plant Journal* **112**, 1014–1028.
- Poucet T, Gonzalez-Moro MB, Cabasson C, Beauvoit B, Gibon Y, Dieuaide-Noubhani M, Marino D. 2021. Ammonium supply induces differential metabolic adaptive responses in tomato according to leaf phenological stage. *Journal of Experimental Botany* **72**, 3185–3199.
- Rasmusson AG, Escobar MA, Hao M, Podgórska A, Szal B. 2020. Mitochondrial NAD(P)H oxidation pathways and nitrate/ammonium redox balancing in plants. *Mitochondrion* **53**, 158–165.
- Sakano K. 2001. Metabolic regulation of pH in plant cells: role of cytoplasmic pH in defense reaction and secondary metabolism. *International Review of Cytology* **206**, 1–44.
- Sarasketa A, González-Moro MB, González-Murua C, Marino D. 2014. Exploring ammonium tolerance in a large panel of *Arabidopsis thaliana* natural accessions. *Journal of Experimental Botany* **65**, 6023–6033.
- Sarasketa A, González-Moro MB, González-Murua C, Marino D. 2016. Nitrogen source and external medium pH interaction differentially affects root and shoot metabolism in *Arabidopsis*. *Frontiers in Plant Science* **7**, 29.
- Scholthof KBG, Irigoyen S, Catalan P, Mandadi KK. 2018. *Brachypodium*: a monocot grass model genus for plant biology. *The Plant Cell* **30**, 1673–1694.
- Setién I, Fuertes-Mendizabal T, González A, Aparicio-Tejo PM, González-Murua C, González-Moro MB, Estavillo JM. 2013. High irradiance improves ammonium tolerance in wheat plants by increasing N assimilation. *Journal of Plant Physiology* **170**, 758–771.
- Shi J, Yi K, Liu Y, *et al.* 2015. Phosphoenolpyruvate carboxylase in *Arabidopsis* leaves plays a crucial role in carbon and nitrogen metabolism. *Plant Physiology* **167**, 671–681.
- Skopelitis DS, Paranychanakis NV, Paschalidis KA, Pliakonis ED, Delis ID, Yakoumakis DI, Kouvarakis A, Papadakis AK, Stephanou EG, Roubelakis-Angelakis KA. 2006. Abiotic stress generates ROS that signal expression of anionic glutamate dehydrogenases to form glutamate for proline synthesis in tobacco and grapevine. *The Plant Cell* **18**, 2767–2781.
- Subbarao GV, Searchinger TD. 2021. A 'more ammonium solution' to mitigate nitrogen pollution and boost crop yields. *Proceedings of the National Academy of Sciences, USA* **118**, e2107576118.
- Swarbreck SM, Wang M, Wang Y, Kindred D, Sylvester-Bradley R, Shi W, Varinderpal-Singh, Bentley AR, Griffiths H. 2019. A roadmap for lowering crop nitrogen requirement. *Trends in Plant Science* **24**, 892–904.
- Takahashi Y, Ebisu Y, Kinoshita T, Doi M, Okuma E, Murata Y, Shimazaki K-I. 2013. bHLH transcription factors that facilitate K⁺ uptake during stomatal opening are repressed by abscisic acid through phosphorylation. *Science Signaling* **6**, ra48.
- Thevenot EA, Roux A, Xu Y, Ezan E, Junot C. 2015. Analysis of the human adult urinary metabolome variations with age, body mass index and gender by implementing a comprehensive workflow for univariate and OPLS statistical analyses. *Journal of Proteome Research* **14**, 3322–3335.
- Tian H, Guo H, Dai X, Cheng Y, Zheng K, Wang X, Wang S. 2015. An ABA down-regulated bHLH transcription repressor gene, bHLH129 regulates root elongation and ABA response when overexpressed in *Arabidopsis*. *Scientific Reports* **5**, 17587.
- Tschoep H, Gibon Y, Carillo P, Armengaud P, Szcwowska M, Nunes-Nesi A, Ferni AR, Koehl K, Stitt M. 2009. Adjustment of growth and central metabolism to a mild but sustained nitrogen-limitation in *Arabidopsis*. *Plant, Cell & Environment* **32**, 300–318.

- Vega-Mas I, Cukier C, Coletto I, González-Murua C, Limami AM, González-Moro MB, Marino D.** 2019a. Isotopic labelling reveals the efficient adaptation of wheat root TCA cycle flux modes to match carbon demand under ammonium nutrition. *Scientific Reports* **9**, 8925.
- Vega-Mas I, Rossi MT, Gupta KJ, González-Murua C, Ratcliffe RG, Estavillo JM, González-Moro MB.** 2019b. Tomato roots exhibit *in vivo* glutamate dehydrogenase aminating capacity in response to excess ammonium supply. *Journal of Plant Physiology* **239**, 83–91.
- von Wittgenstein NJ, Le CH, Hawkins BJ, Ehling J.** 2014. Evolutionary classification of ammonium, nitrate, and peptide transporters in land plants. *BMC Evolutionary Biology* **14**, 11.
- Vos PG, Paulo MJ, Voorrips RE, Visser RG, van Eck HJ, van Eeuwijk FA.** 2017. Evaluation of LD decay and various LD-decay estimators in simulated and SNP-array data of tetraploid potato. *Theoretical and Applied Genetics* **130**, 123–135.
- Wang J, Hüner N, Tian L.** 2018. Identification and molecular characterization of the *Brachypodium distachyon* *NRT2* family, with a major role of *BdNRT2.1*. *Physiologia Plantarum* **165**, 498–510.
- Wang J, Zhang Z.** 2021. GAPIT Version 3: boosting power and accuracy for genomic association and prediction. *Genomics, Proteomics & Bioinformatics* **19**, 629–640.
- Xiao C, Fang Y, Wang S, He K.** 2023. The alleviation of ammonium toxicity in plants. *Journal of Integrative Plant Biology* **65**, 1362–1368.
- Xie Y, Lv Y, Jia L, et al.** 2023. Plastid-localized amino acid metabolism coordinates rice ammonium tolerance and nitrogen use efficiency. *Nature Plants* **9**, 1514–1529.
- Zhang N, Gibon Y, Wallace JG, et al.** 2015. Genome-wide association of carbon and nitrogen metabolism in the maize nested association mapping population. *Plant Physiology* **168**, 575–583.